

1 **Complement pathway gene activation and rising circulating immune complexes**
2 **characterize early disease in HIV-associated tuberculosis**

3
4 **Authors:** Hanif Esmail^{1,2,3*}, Rachel P. Lai⁴, Maia Lesosky^{2,5}, Katalin A. Wilkinson^{2,4}, Christine
5 M. Graham⁶, Stuart Horswell⁴, Anna K. Coussens^{2, 7}, Clifton E. Barry 3rd^{2,8,9,10}, Anne
6 O'Garra^{6,11}, Robert J. Wilkinson^{1,2,4*}

7
8 **Affiliations:**

9 ¹ Department of Medicine, Imperial College London, W2 1PG, United Kingdom

10 ² Wellcome Center for Infectious Diseases Research in Africa, Institute of Infectious Disease and
11 Molecular Medicine and Department of Medicine, University of Cape Town, Observatory 7925,
12 Republic of South Africa

13 ³ Radcliffe Department of Medicine, University of Oxford, Oxford, United Kingdom

14 ⁴ The Francis Crick Institute, London, NW1 2AT United Kingdom

15 ⁵ Division of Epidemiology and Biostatistics, School of Public Health and Family Medicine,
16 University of Cape Town, Cape Town, Republic of South Africa

17 ⁶ The Francis Crick Institute, Laboratory of Immunoregulation and Infection, London, NW1 2AT
18 United Kingdom

19 ⁷ Division of Medical Microbiology, Department of Pathology, University of Cape Town,
20 Observatory 7925, Republic of South Africa

21 ⁸ Faculty of Medicine and Health Sciences, Stellenbosch University, Cape Town, Republic of
22 South Africa

23 ⁹ Tuberculosis Research Section, NIAID, NIH, Bethesda, USA

24 ¹⁰ Department of Clinical Laboratory Sciences, University of Cape Town, Cape Town, Republic
25 of South Africa

26 ¹¹ National Heart and Lung Institute, Imperial College London, W2 1PJ, United Kingdom

27 *To whom correspondence should be addressed: hanif.esmail@ndcls.ox.ac.uk and
28 r.j.wilkinson@imperial.ac.uk

29 **Competing interests:**

30 The authors have no competing interests to declare

31

32 **Significance statement**

33 Understanding the events in early tuberculosis disease will facilitate the development of novel
34 tests to predict disease progression and interventions to prevent it. Blood-based transcriptomic
35 approaches consistently identify several pathways relevant to clinical disease. Here we show in
36 asymptomatic people with HIV infection and early subclinical tuberculosis defined by FDG-
37 PET/CT, that transcripts relating to the classical complement pathway and Fc γ -receptor remain
38 enriched, accompanied by rising levels of circulating antibody/antigen immune complexes. We
39 confirm that transcripts relating to these pathways also rise in the 12 months prior to disease
40 presentation in HIV-uninfected people. This supports observations that antigen may be present
41 in early disease despite being paucibacillary, and demonstrates that modulation of the immune
42 response could occur via immune complex formation.

43

44

45

46

47 **Abstract**

48 The transition between latent and active tuberculosis (TB) occurs prior to symptom onset. Better
49 understanding of the early events in subclinical disease will facilitate the development of
50 diagnostics and interventions that improve TB control. This is particularly relevant in the
51 context of HIV-1 co-infection where progression of TB is more likely.

52

53 In a recent study using [¹⁸F]-fluoro-2-deoxy-D-glucose positron emission/computed tomography
54 (FDG-PET/CT) on 35 asymptomatic, HIV-1 infected adults we identified ten participants with
55 radiographic evidence of subclinical disease, significantly more likely to progress than the 25
56 participants without. To gain insight into the biological events in early disease we performed
57 blood-based whole genome transcriptomic analysis on these participants and 15 active TB
58 patients. We found transcripts representing the classical complement pathway and Fcγ receptor-
59 1 overabundant from subclinical stages of disease. Levels of circulating immune
60 (antibody/antigen) complexes also increased in subclinical disease and were highly correlated
61 with C1q transcript abundance. To validate our findings, we analyzed transcriptomic data from a
62 publicly available dataset where samples were available in the 2 years prior to TB disease
63 presentation. Transcripts representing the classical complement pathway and Fcγ receptor-1
64 were also differentially expressed in the 12 months prior to disease presentation.

65

66 Our results indicate that levels of antibody/antigen complexes increase early in disease,
67 associated with increased gene expression of C1q and Fcγ receptors that bind them.
68 Understanding the role this plays in disease progression may facilitate development of

69 interventions that prevent this leading to a more favorable outcome and may also be important to
70 diagnostic development.

71

72 /body

73 **Introduction**

74 Conventionally, tuberculosis (TB) is divided into stages of asymptomatic latent infection, during
75 which bacillary replication is effectively controlled in a healthy host, and active disease in which
76 this has failed, resulting in symptomatic deterioration. Understanding the transition between
77 these two states is important, although until recently this has been over-looked (1). Active
78 disease is usually defined by a combination of symptoms, pathology (radiographically or
79 histologically identified) and culturable bacilli. These features do not appear simultaneously but
80 develop over time and may be intermittently present, hence the active disease processes may
81 begin months before symptom onset i.e. as subclinical active disease (2). In some of those who
82 initially reactivate, disease progression may be arrested and regress particularly when disease
83 extent is limited(3). A greater understanding of the early events in disease is critical for the
84 development of novel approaches to both identify people in early subclinical stages of disease
85 and interventions to prevent progression. This is of particular importance in those with HIV-1
86 co-infection where TB disease progression is more likely. However, studying the natural history
87 of TB in this group is further complicated by the imperative to provide preventive therapy, so
88 novel approaches are needed.

89

90 In macaques the failure of the granuloma has been shown to be followed by cellular infiltration
91 within bronchi (pneumonia)(4). In human autopsy studies pneumonic infiltration has also been

92 observed as the first pathological sign of pulmonary disease(5). Disease regression and self-
93 healing of lesions is associated with fibrosis, however, it appears that disease risk following this
94 is significantly increased(6). Medical imaging is a key approach to detecting evidence of early
95 disease in asymptomatic persons, facilitated by a characteristic distribution of pathology. Chest
96 radiography (CXR) has long been used for this purpose, however, CXR has limitations in both
97 sensitivity and reproducibility(7). [¹⁸F]-fluoro-2-deoxy-D-glucose positron emission/computed
98 tomography (FDG-PET/CT) is a highly sensitive imaging modality, which combines cross-
99 sectional anatomical detail from a CT scan with quantitation and localization of metabolic
100 activity by quantifying uptake of FDG (a glucose analogue) by PET scan. FDG uptake in
101 tuberculosis is related to activated macrophages and an inflammatory infiltrate at the site of
102 disease(8). In a recent clinical study, we utilized FDG-PET/CT to identify evidence of early
103 disease in asymptomatic people otherwise conventionally considered to have latent infection
104 (QuantiFERON Gold in-tube (QF-GIT) positive, sputum culture negative, CXR no evidence of
105 active disease) but at high risk of disease progression as HIV-1 infected, anti-retroviral therapy
106 naïve. Of the 35 people scanned 10 (28.6%) had evidence of subclinical disease by FDG-
107 PET/CT and they were significantly more likely to progress to clinical disease(2).

108

109 Transcriptomic profiling of peripheral blood has provided critical insight into active TB (9-12).
110 Blankley *et al* have recently analyzed 16 such studies and shown overall findings in modular
111 analysis of the transcriptome to be remarkably consistent. Meta-profiling identified 380 genes
112 differentially abundant in active TB in at least 9 of the 16 studies. Based on pathway analysis
113 they then determined the main functional groups of genes in active TB to relate to; Interferon
114 signaling/inducible genes, the complement pathway, immunoglobulin receptors, recognition of

115 pathogen associated molecular patterns, inflammasome and pro-inflammatory pathways, (13,
116 14). However, it is not clear which of these processes occur at the earliest stages of disease.
117 Understanding such host-pathogen interaction in early disease may provide insight that could
118 facilitates novel approaches to diagnose and manage subclinical disease. *Zak et al* have recently
119 demonstrated in HIV-1 uninfected adolescents that transcriptional differences are present in
120 blood months prior to clinical patency suggesting that transcriptomic profiling of peripheral
121 blood might be a useful approach to provide insight into subclinical disease.

122

123 In the present study, we utilized the cohort of HIV-1 infected adults described above in which
124 presence or absence of subclinical TB was defined by FDG-PET/CT(2) and co-recruited control
125 participants with active TB. We investigated which components of the active TB whole blood
126 transcriptional profile were present in those with evidence of subclinical disease to provide
127 insight into the biology underlying early progressive disease.

128

129 **Results**

130 Details of the clinical and radiographic features of the clinical cohort have been previously
131 described(2). Thirty-five asymptomatic, healthy, HIV-1 infected, ART naïve participants with
132 median CD4 count of 517/mm³, a positive QFN-GIT and no previous history of TB, were
133 screened for active TB by two sputum cultures (induced if needed) and CXR. All participants
134 were of African ancestry resident in Khayelitsha (township of Cape Town, South Africa).
135 Following 42-day negative sputum cultures, participants were confirmed as remaining symptom
136 free, underwent FDG-PET/CT and were commenced on isoniazid preventive therapy. FDG-
137 PET/CT scans were systematically analyzed, with abnormalities categorized and spatially

138 mapped, interpreted in the context of historical autopsy studies and then classified as being
139 consistent with subclinical active TB or not. Ten of the 35 participants were classified as having
140 subclinical active TB, due to either infiltrates and/or fibrotic scars (n = 9 – consistent with
141 bronchogenic spread of disease) or multiple active nodules (n = 1 – consistent with
142 haematogenous spread of disease) on FDG-PET/CT (referred to as “subclinical TB”); the
143 remaining 25 participants had no evidence of disease activity on FDG-PET/CT scan (referred to
144 as “latent TB”). Four out of 10 participants with evidence of subclinical TB were determined to
145 have disease progression (defined as developing TB symptoms along with radiographic
146 deterioration or culture positivity) requiring commencement of standard TB therapy in contrast
147 to 0/25 participants with no evidence of subclinical TB. Participants were followed up for 6
148 months, 27 of 35 participants (six subclinical and 21 latent) then had repeat FDG-PET/CT. All
149 six of the subclinical participants had improvement in baseline abnormalities in lymph nodes and
150 lung parenchyma in contrast to only 1/21 of those without evidence of subclinical TB. Three
151 participants (2 in subclinical group and 1 in the latent group) had been commenced on
152 antiretroviral therapy during follow up as CD4 count fell below $350/\text{mm}^3$, in accordance with
153 local standard of care at the time of recruitment.

154 In addition, we recruited 15 participants with symptomatic, microbiologically confirmed
155 pulmonary TB (referred to as “active TB”) for blood sampling. There were no significant
156 differences between those with active, subclinical and latent TB with regard to median age
157 ($p=0.41$), sex ($p=0.52$) or median CD4 count ($p=0.09$). Conversely, median viral load (VL) and
158 median C-reactive protein (CRP) were significantly different between active and latent TB
159 ($p<0.0001$ and $p=0.0001$; respectively), but not between subclinical and latent TB ($p=0.97$ and
160 $p=0.08$ respectively) (**SI Appendix, Figure S1**).

161

162 *Eighty-two transcripts distinguish subclinical and active TB from latent TB*

163 Transcript abundance in whole blood RNA was determined by Illumina HumanHT-12 v 4.0
164 Expression BeadChips microarray. We initially defined a set of transcripts that were
165 differentially abundant between latent and active TB to determine a transcriptional profile of
166 active TB. From the 47,231 probes on the microarray, 18,919 were present in at least 10% of
167 samples (see methods). The 18919 transcripts were then statistically filtered (ANOVA with
168 Benjamini Hochberg FDR correction ($p_{\text{corr}} < 0.05$) to identify 2573 transcripts showing
169 significant differential abundance between the different stages of TB. From these transcripts, we
170 identified 893 transcripts with at least a 1.5-fold difference in abundance between active and
171 latent TB. To determine which of these transcripts might be relevant to early disease, we filtered
172 the 893 transcripts by fold change to identify those differentially abundant between subclinical
173 and latent TB. As disease pathology in subclinical TB is of minimal extent by comparison with
174 active TB, we reasoned that the relevant transcripts may be expressed in blood at lower levels in
175 comparison to active TB and hence both 1.25 and 1.5-fold change cut offs were used resulting in
176 a 203 and 82-transcript list respectively (**SI Appendix, Figure S2 and Supp. Excel sheet**).

177

178 Hierarchical clustering was then performed on the 893, 203 and 82 transcripts which confirmed
179 progressive improvement in ability to classify those with subclinical TB from those with latent
180 TB while clustering them with active TB (**Figure 1a**). Two participants with subclinical TB did
181 not cluster with active TB, one with multiple active nodules consistent with haematogenous
182 spread of disease and the other who, of those with abnormalities consistent with bronchogenic
183 spread, had the smallest infiltrate with amongst the lowest metabolic activity in lesion or lymph

184 node by FDG uptake (**SI Appendix, Table S1**). In 27 participants seen at 6-month follow-up
185 after receiving either IPT or standard TB therapy the subclinical and latent groups became
186 indistinguishable by transcriptional signature (**Figure 1b**).

187
188 To examine if abundance of these transcripts altered as subclinical disease activity increased we
189 investigated the association of metabolic activity by FDG uptake with transcript abundance.
190 Participants with subclinical TB were further divided into two categories; five participants
191 showing intense FDG uptake (Visual score (VS) =3) within lung parenchyma or central lymph
192 nodes and five participants with less intense FDG uptake (VS=0-2) (**SI Appendix, Table S1**).
193 Hierarchical clustering using the group mean expression values for the 82-transcripts
194 demonstrated that the subclinical participants with greater metabolic activity, clustered more
195 closely with active TB than the subclinical TB group with low FDG uptake, which in turn
196 clustered closer to the latent TB group (**Figure 1c**). This was then further demonstrated by
197 disease risk score (determined for each participant by subtracting the summed normalized
198 expression values of under-abundant transcripts from that of over-abundant transcripts as
199 described in (12)) (**Figure 1d**). There was no significant difference in mean C-reactive Protein
200 (CRP) (2.62 mg/L vs 2.88 mg/L; $p=0.85$ – Normal range <5 mg/L), white cell count (WCC)
201 ($5.72 \times 10^9/L$ vs $5.77 \times 10^9/L$; $p=0.97$ – Normal range $4.5-11 \times 10^9/L$) or Log (HIV VL
202 (copies/mL)) (4.29 vs 4.36; $p=0.86$) between the participants with subclinical TB as high or low
203 metabolic activity on PET/CT.

204
205 To evaluate if HIV-1 viral load contributed the observed differential abundance between TB
206 disease states in the 82-transcript signature, we performed multiple regression using TB status
207 (latent, subclinical, active) and HIV viral load as explanatory variables for expression score. TB

208 status but not HIV VL was significantly associated ($r^2=0.75$, $p<0.0001$; TB status, $\text{coef}=55.9$,
209 $p<0.001$; HIV VL, $\text{coef}=9.18$, $p=0.08$).

210 The 893, 203 and 82 transcripts mapped to 678, 181 and 72 genes respectively, of these 174, 39
211 and 17 genes respectively are present in the 380 meta-gene signature for active TB, identified by
212 Blankley *et al* as being present in at least 9 other studies hence consistently associated with
213 TB(13), (**SI Appendix, Table S2 and Supp. Excel sheet**).

214

215 *Classical complement pathway transcripts are overabundant in subclinical disease and correlate*
216 *with the concentration of circulating immune complexes*

217 To identify biological processes common to subclinical and active TB, pathway analysis was
218 performed on the three transcript signatures (893, 203 and 82). In the 893-transcript active TB
219 signature showed complement and interferon signaling to be the most enriched canonical
220 pathways (each, $p=0.0002$), followed by death receptor signaling and JAK family kinase in IL-6
221 signaling (**Figure 2a**). Of these, only complement remained over-represented in the 203 and 82-
222 transcript signatures ($p=0.0001$ and $p=0.006$ respectively) suggesting that complement may be
223 relevant in early active disease. Using only the 174, 39 and 17 genes common to the 380-meta
224 signature this pattern was retained with complement remaining the most enriched pathway in all
225 3 gene lists (**SI Appendix, Figure S4**)

226

227 Predominantly components of the classical complement pathway (complement component 1q
228 subcomponent B (C1QB), serpin peptidase inhibitor member 1 (SERPING1), complement
229 component 2 (C2) and complement component 5 (C5)) were overabundant in the blood of
230 subclinical and active TB patients compared to those with latent TB (**Figure 2b**). Of these

231 C1QB, SERPING1 and C2 are all in the 380-metاسignature derived by Blankley *et al*, with
232 C1QB and SERPING1 being overabundant in active TB for 15 of the 16 studies analyzed.
233 To further investigate the role of complement in subclinical TB, we next evaluated the
234 relationship between serum concentration of complement proteins C1q, SERPING1 and C5 and
235 their whole blood transcript abundance using paired samples. There was no correlation between
236 serum concentration and transcript abundance for C1q ($r_s=-0.08$, $p=0.59$), SERPING1 ($r_s=0.02$,
237 $p=0.89$) or C5 ($r_s=0.16$, $p=0.29$) (**Figure 3a, c, e**). Because the classical complement pathway is
238 triggered by C1q binding of antibody/antigen immune complexes(15), we next evaluated the
239 relationship between transcript abundance of C1QB and serum concentration of circulating
240 immune complex (CIC – antibody/antigen complexes) as determined by a C1q binding assay.
241 Transcript abundance of C1QB in whole blood was significantly correlated with CIC ($r_s=0.48$,
242 $p=0.0005$) as was SERPING1 ($r_s=0.46$, $p=0.0008$) but not C5, where a trend was observed albeit
243 not significant ($r_s=0.26$, $p=0.08$) (**Figure 3b, d, f**). As both TB and HIV can contribute to levels
244 of CIC we performed multiple regression by TB status (latent, subclinical, active) and HIV viral
245 load as explanatory variables for CIC. TB status but not HIV VL had a significant association
246 ($r^2=0.26$, $p=0.001$; HIV VL, $\text{coef}=0.10$, $p=0.25$; TB status, $\text{coef}=0.31$, $p=0.008$).

247

248 We next evaluated the relationship between CIC and metabolic activity in subclinical TB
249 classifying participants as having low or high metabolic activity as above. CIC was significantly
250 increased across different TB disease states ($p=0.0004$), *post hoc* analysis controlling for false
251 discovery demonstrated that those with active TB ($p=0.0001$, $q=0.0002$) and those with
252 subclinical TB and high metabolic activity on PET/CT ($p=0.038$, $q=0.04$) had higher serum
253 concentration of CIC than latent TB (**Figure 3g**). Furthermore serum CIC as a single marker to

254 discriminate the four individuals subsequently treated for TB during follow-up from the 31
255 individuals that were not, showed an AUC of 0.754. A cut off of 192 $\mu\text{g Eq/ml}$ had sensitivity of
256 75% and specificity of 93.6% and correctly classified 91.4%. Of note the only participant of the
257 four subsequently treated for active TB with a serum CIC less than 192 $\mu\text{g Eq/ml}$ had a different
258 radiographic presentation subclinical disease, with multiple nodules suggestive of
259 haematogenous spread in contrast to the bronchogenic pattern of disease seen in the remainder.

260
261 In addition to binding C1q, antibody/antigen immune complexes also bind Fc γ receptors and Fc γ
262 Binding Protein (FCGBP). Those with subclinical TB and active TB also had relative
263 overabundance of transcripts relating to the Fc fragment of IgG, high affinity I receptor (CD64)
264 (FCGR1) with FCGR1A/B/C all being present in the 82 and/or 203 transcript list, however there
265 was a reduction in abundance of FCGBP (**Figure 2c and SI Appendix, Table S2**). FCGR1A,
266 FCGR1B and FCGBP were all present in the 380 meta-signature. FCGBP is the most
267 consistently underabundant transcript in active TB identified in 14 previous studies. By contrast
268 FCGR1B and FCGR1A are amongst the most consistently overabundant transcripts in active TB
269 being present in 16 and 14 studies respectively. RT-PCR was also conducted using primers for
270 FCGR1C, FCGBP, C1QB and SERPING1 which confirmed the differences demonstrated by
271 microarray between latent, subclinical and active TB (**SI Appendix, Figure S3**).

272
273 *Classical complement and interferon signaling pathways are increased in progressive TB in HIV*
274 *uninfected persons*

275 To validate our findings and establish if classical complement and Fc gamma receptor gene
276 activation were important in early TB disease, we reanalyzed the RNA sequencing data from the

277 publically available dataset from the study reported by Zak *et al*, in which, samples were
278 available in the 2 years prior to disease presentation with appropriate non-progressor
279 controls(16). Although no accurate subclinical disease phenotype was ascertained, we reasoned
280 that those in the 6 to 12 months prior to disease presentation may have had subclinical disease.
281 Furthermore, participants in Zak *et al* were all HIV uninfected allowing us to determine whether
282 our findings were generalizable. To investigate the biological processes relevant to progressing
283 disease, we first established the number of transcripts significantly differentially abundant (p_{corr}
284 <0.05) and with $>1.5\text{FC}$ overabundance between progressors and non-progressors at <180 days,
285 181-360 days, 361-540 days and 541-720 days prior to disease presentation, identifying 362,
286 154, 3 and 3 genes respectively (**see methods and Supp. Excel sheet**). We then conducted IPA
287 analysis for the <180 day and 181-360 time points. The complement pathway was the second and
288 third most significantly enriched canonical pathway at 181-360 days ($p=5.80\times 10^{-5}$ (11.1% of
289 pathway, $p=5.80\times 10^{-5}$) and <180 days prior to presentation ($p=6.02\times 10^{-7}$ (19.4% of pathway,
290 $p=6.02\times 10^{-7}$) respectively, with the interferon signaling pathway the most significantly enriched
291 at these time points (Figure 4). In keeping with our initial results, the classical complement
292 pathway was largely responsible for this with C1QB/C, SERPING1 and C2 all significantly
293 differentially expressed at both time points and C5 and C1QA also significantly differentially
294 expressed <180 days before presentation. In addition, FCGR1A/B/CP were all amongst the most
295 significantly differentially expressed genes between progressors and non-progressors at both
296 time points (all in top 22 genes for both) (**Figure 4**).

297

298 *Interferon signaling transcripts are increased in both untreated HIV and active TB*

299 Enrichment of the complement pathway was observed in early TB disease states in both HIV-
300 infected and un-infected persons, however, enrichment of interferon signaling was less
301 prominent in HIV-associated TB. We further explored this by undertaking a modular analysis of
302 the whole blood transcriptome in HIV and active TB. Modules are groups of co-regulated
303 transcripts subsequently categorized into functional groups through unbiased literature review.
304 The principles informing this approach have been previously published (17). Using this
305 approach, the modular profile of active TB has been previously shown to be remarkably
306 consistent across 16 studies (13).

307
308 For this analysis, in addition to the HIV-1 infected, ART naïve participants with symptomatic
309 active pulmonary TB (HIV+ART-TB+; n=15) and with no evidence of active TB (HIV+ART-
310 TB-; n=25, i.e. excluding the 10 with subclinical active TB), we recruited HIV uninfected
311 participants with symptomatic, active, pulmonary TB (HIV-TB+; n=14) and with no evidence of
312 active TB (HIV-TB-; n=15). We also recruited HIV-1 infected participants established on ART
313 fully with viral load fully suppressed and no evidence of active TB (HIV+ART+TB-; n=8). All
314 these additional participants were also resident Khayelitsha and of African ancestry.

315
316 18,751 transcripts were “present” in at least 10% of samples and included in the modular
317 analysis, using HIV-TB- participants as the primary control group. The average transcript
318 abundance for each module was determined for each participant. Of the 260 modules previously
319 characterized, 38 had functional roles determined and analysis was restricted to these modules,
320 three of these modules relate to interferon signaling.

321

322 By comparison HIV-TB- participants, participants with untreated HIV only (HIV+ART-TB-)
323 had significant differences (after correcting for false discovery) in modular expression in 8/38
324 modules (5 increased expression and 3 reduced expression), those with TB only (HIV-TB+) had
325 significant differences in expression in 24/38 modules (15 increased expression and 9 reduced
326 expression) (**SI Appendix, Table S3**). Both the HIV only group and TB only group had
327 significantly increased expression in all three interferon modules. Those with HIV-associated
328 TB (HIV+ART-TB+) had greater expression of the interferon modules in comparison to those
329 with HIV or TB only (**Figure 5 and SI Appendix, Table 3**). Those with HIV but on ART
330 (HIV+ART+TB-) with fully suppressed viral load showed normalization of expression within
331 the interferon modules and had no significant differences in any of the 38 modules in comparison
332 to HIV-TB- controls. Given the background increased abundance of interferon related
333 transcripts in HIV infected persons not on ART it is likely that any increases expression within
334 these pathways in early tuberculosis would be less discriminatory.

335
336 Recognizing that interferons are well known to enhance expression of Fcγ receptor we next
337 sought to establish the effect of interferon on expression of complement components. We cross-
338 referenced the 36 genes comprising the Ingenuity IPA complement canonical pathway against
339 the Interferome database, a database of interferon regulated genes (IRG) from a variety of
340 experimental settings (<http://www.interferome.org/interferome/home.jsp>). All human data on
341 IRG were from *in vitro* experiments, we restricted analysis to studies on human blood and genes
342 showing > 2-fold increase following interferon stimulation. Of the 36 genes, 9 (25%) had
343 evidence of increased expression on interferon stimulation; C1QA/B/C, C2, CFB, CR1, CR2,
344 ITGAX SERPING1. While abundance of some of these potentially interferon regulated

345 complement components were enriched in tuberculosis others were not, in addition C5 did not
346 have experimental evidence of interferon regulation. Furthermore overall abundance of
347 transcripts relating the to the TB relevant complement and FCGR1 components (C1QA/B/C,
348 SERPING1, C2, C5, FCGR1A/B/C) while significantly increased in TB, was not significantly
349 affected by HIV status (two-way ANOVA with TB and HIV as explanatory variables of disease
350 risk score; r^2 0.58, TB $p < 0.0001$ and HIV $p = 0.12$) with discriminatory ability of these transcripts
351 for TB in both HIV infected and uninfected persons excellent (disease risk score; HIV infected -
352 AUC 0.997, HIV uninfected – AUC 0.938) (**SI Appendix, Figure S5**). It is therefore unlikely
353 that the complement pathway member upregulated in TB merely reflect interferon responsive
354 genes.

355
356 To establish if this pattern of complement and FCGR transcript expression was seen in other
357 diseases we analysed the dataset (GEO dataset- GSE42834) of Bloom et al in which participants
358 with active TB, active sarcoid, non-active sarcoid, lung cancer, pneumonia and healthy controls
359 had whole blood transcriptional profiling undertaken(18). We profiled transcript abundance of
360 the 81 complement and FCGR transcripts (62 transcripts relating to the 36 complement genes in
361 the IPA database and all 19 FCGR transcripts on the platform). 19 of 81 transcripts showed
362 greater than 2-fold difference in transcript abundance in at least one of the disease categories
363 when compared to healthy controls. In initial hierarchical clustering of disease groups for these
364 19 transcripts showed active TB clustered with active sarcoid, and community-acquired
365 pneumonia clustered with lung cancer (**SI Appendix, Figure S6**). We then performed K-means
366 clustering (3 clusters, 50 iterations, Euclidean distance metric) to provide an unbiased assessment
367 of the pattern of transcript abundance across the different diseases. One cluster contained

368 transcripts showing greatest abundance in tuberculosis over other diseases included C1QB,
369 SERPING1, FCGR1A, FCGR1B and FCGR1C. The cluster containing transcripts showing
370 greatest abundance in diseases other than tuberculosis (particularly pneumonia and lung cancer)
371 included CR1, ITGAM, ITGAX, C3AR1, FCGR2A and FCGR3B. The final cluster contained
372 FCGRBP as a single transcript that was under abundant in tuberculosis, community-pneumonia
373 and lung cancer in comparison to control. These data support our findings of complement and
374 FCGR expression in tuberculosis, demonstrated in other cohorts presented in the paper and also
375 re-emphasis, that complement component expression is not simply a function of interferon
376 stimulation or a generic inflammatory signal.

377

378 **Discussion**

379 We have previously shown that in a subgroup of asymptomatic, HIV-1 infected persons,
380 conventionally diagnosed with latent TB, evidence of subclinical disease can be identified
381 utilizing high resolution imaging (FDG-PET/CT) which is not apparent by routine clinical
382 screening. Those with evidence of subclinical disease on FDG-PET/CT were also found to be
383 more likely to progress clinically and to require treatment for active TB (2). In this study we
384 have identified components of the active TB whole blood transcriptional response that are also
385 present in subclinical disease and shown that circulating immune complexes rise during
386 subclinical disease.

387

388 Previous transcriptional studies have consistently indicated several key pathways in active TB
389 (interferon signaling/inducing genes, inflammasome/pro-inflammatory pathways, recognition of
390 PAMP, the complement pathway and immunoglobulin receptors) but these studies have not been

391 able to dissect the biological processes that may occur at the outset of disease. We determined
392 that a subset of transcripts in the whole blood transcriptional response to symptomatic active TB
393 were relevant to subclinical disease and that these transcripts were enriched for the classical
394 complement pathway and immunoglobulin receptors (FC γ receptor 1), suggesting a cellular
395 response to antibody-antigen complexes may occur early in disease. This was supported by our
396 finding that CIC in serum increased in relation to TB disease status and was highly correlated
397 with transcript abundance of C1q. Furthermore, with increasing metabolic activity of subclinical
398 disease the transcriptional response aligned more closely with active TB and levels of CIC
399 increased. Importantly the abundance of these transcripts and levels of CIC did not show any
400 significant relationship with HIV viral load.

401
402 We validated our findings utilizing the publicly available data reported by Zak *et al* (16). While
403 subclinical disease was not characterized by imaging, regular samples were available up to 2
404 years prior to clinical disease presentation in HIV uninfected persons. Of note in contrast to our
405 study, Zak *et al* also excluded participants who developed TB within 6 months of enrolment in
406 the training set and 3 months of enrolment in the validation set. Our analysis confirmed that
407 transcripts relating to the classical complement pathway and immunoglobulin receptors increased
408 during the 12 months prior to disease presentation in HIV uninfected persons. However, in
409 addition interferon signaling pathways also appear to increase in this population. Whilst
410 interferon-signaling pathways were prominent in our 893-transcript signature differentiating
411 active from latent TB in HIV infected persons they became less prominent as this signature was
412 filtered to allow better distinction of subclinical TB from latent TB. We showed that untreated
413 HIV infection itself leads to increases in interferon related transcripts in whole blood. Hence, the

414 finding that the interferon signaling pathway transcripts were less discriminatory in early disease
415 in those with untreated HIV is likely due to the high background level of these transcripts in this
416 population. We also showed that the pattern of complement and FCGR expression varied in
417 different pulmonary diseases. While the pattern of expression in tuberculosis was also seen in
418 active sarcoidosis though at a lower level of expression, a different pattern of expression was
419 seen in community-acquired pneumonia and lung cancer where expression of C3 binding
420 receptors was more prominent. Tuberculosis and sarcoidosis have previously been shown to
421 have many similarities in whole blood transcriptional profile(18, 19).

422

423 Transcripts relating to the classical complement pathway (in particular, C1Q and SERPING1)
424 and Fcγ Receptor 1 are amongst the most consistently overabundant in active TB and FCGBP as
425 the most consistently underabundant supporting their role in early disease. Cliff *et al* also
426 reported that transcripts relating to the complement pathway decrease within the first week of
427 treatment for active TB(20). This suggests that the abundance of transcripts relating to the
428 complement pathway may mark a rising antigen load rising early in disease, falling rapidly with
429 treatment. CIC has frequently been reported to be elevated in active tuberculosis, increasing
430 with extent of disease and reducing with treatment, CIC have been shown to contain secreted TB
431 antigens (e.g. 38kDa and 30kDa (Ag85)) and non-secreted antigens (e.g. 16kDa (HspX)) (21,
432 22). In addition to opsonisation and complement activation, antibodies have an additional
433 functional role in regulating the immune response through interaction with innate cells via a
434 variety of Fc Receptors which may directly affect effector mechanisms and clearance of the
435 pathogen (23-25).

436

437 Hunter *et al* investigated the histological appearances of early pulmonary TB in humans in
438 several studies. They demonstrated that the earliest feature of disease is a lipid-rich pneumonia
439 in which alveoli are filled with foamy macrophages with CD4 cells present at significantly lower
440 frequency than in the granuloma. They also observed large clusters of B-cells bordering this
441 region. Very few acid-fast bacilli (AFB) are visible at this stage but abundant mycobacterial
442 antigen is evident on immunohistochemical staining. As necrosis develops within the pneumonia
443 there is then a marked increase in numbers of AFB (26-28). Increased concentration of both
444 38kDa TB antigen and 38kDa specific IgG have been identified in bronchoalveolar lavage
445 samples of TB patients(29).

446

447 Based on our findings we propose that at this early stage of disease, the increase in
448 mycobacterial antigen concentration results in an increased concentration of antibody-antigen
449 complexes increases at the site of disease. This may lead to increased expression of components
450 of the classical complement pathway in recruited cells (to facilitate the targeted delivery of
451 complement) and up-regulation of Fc γ receptor on monocytes and neutrophils to promote
452 phagocytosis, as we have observed. By contrast expression of FCGBP is reduced. FCGBP has
453 been shown to be the most consistently underabundant gene in active compared to latent TB but
454 little is known about its function. Kobayashi *et al* have shown that Fc γ Binding Protein is
455 present in sputum as well as other bodily secretions and that it inhibits activation of classical
456 complement pathway(30). Its reduction in TB disease may therefore facilitate C1q binding of
457 immune complexes promoting complement activation.

458

459 Formation of immune complexes in disease has both beneficial and detrimental effects for the
460 host and the complement system can both promote and mitigate immunopathology. Immune
461 complex aggregates that precipitate and persist within the lung are likely to be damaging through
462 C3a/C5a mediated neutrophil recruitment increasing inflammation and tissue necrosis which
463 may promote bacillary multiplication(31). It has been suggested that solubilization and diffusion
464 of immune complexes away from tissue via extracellular fluid and the systemic circulation for
465 clearance by mononuclear phagocytic system is critical to minimize local inflammation and
466 tissue damage (32, 33). This appears to be facilitated by rapid C1q initiation of the classical
467 complement pathway and C3b deposition which results in reduction in the size of the immune
468 complex aggregates to maintain solubility, deficiencies in classical complement components
469 reduce immune complex solubility and increase risk of immune complex mediated autoimmune
470 diseases (32, 33). It is possible, therefore, that the increased expression of classical complement
471 components in tuberculosis is directly in response to increased production of immune complexes
472 at the site of disease to allow localized delivery of C1q to inhibit the precipitation of immune
473 complexes and minimize lung damage. Although, our insight has been informed by analysis of
474 blood, Cai *et al* demonstrated that C1q mRNA and protein levels were greater at the site of
475 disease (in pleural fluid and bronchoalveolar lavage fluid) compared to blood in active pleural
476 and pulmonary tuberculosis (34).

477

478 We found that although abundance of classical complement components correlated with
479 circulating immune complexes they did not correlate well with serum levels of the proteins they
480 encode. There are several possible explanations of this. For blood cells migrating to the disease
481 site, expression as well as consumption of complement may occur locally. In addition,

482 complement components may also be bound to immune complexes whereas the assay would
483 only measure unbound complement proteins. Furthermore, whole the blood transcriptome
484 predominantly reflects mRNA expression in leukocytes whereas circulating complement proteins
485 are manufactured within the liver and by a number other cell types (e.g. epithelial and
486 endothelial cells) affecting the correlation of whole blood RNA and serum protein(35).

487
488 There are limitations of this study. We used a broad definition of subclinical disease which
489 grouped together several distinct abnormalities found to be consistent with early disease, with
490 reference to historical autopsy studies. Our sample size was modest and participants often had a
491 combination of abnormalities and hence we were unable to tease out transcriptional differences
492 between participants with potentially different disease pathogenesis. For example, there may be
493 differences between those presenting with multiple nodules suggestive of haematogeneous
494 spread of disease in comparison to disease spreading bronchogenically which may be interesting
495 the characterize. Larger studies will be needed explore this in greater detail and further validate
496 findings. In addition, we used peripheral blood to investigate pathogenesis of disease, while this
497 approach is widely adopted, confirmation of our findings is needed in samples from site of
498 disease. Our study was conducted in ART naïve, HIV infected participants with well-preserved
499 CD4 counts with validation in HIV uninfected adolescents, confirmatory studies in other
500 populations are required. Furthermore, although we demonstrated that CIC rises in relation to
501 disease state in tuberculosis. This may have a role as a biomarker for identification of subclinical
502 disease, however further studies will be needed confirm these findings in independent cohorts.

503

504 Our results indicate that the abundance of transcripts relating to the classical complement
505 pathway and Fc γ receptors is increased from early disease in both untreated HIV infected adults
506 and HIV uninfected adolescents in contrast to transcripts related to interferon signaling which
507 appear less discriminatory in untreated HIV infected people. This will be an important
508 consideration in the development of universal transcript-based biomarkers that are predictive of
509 disease. Our findings support the observation that in early disease, though paucibacillary,
510 antigen may still be present. This may have the potential to modulate the immune response by
511 forming antibody complexes that initiate the complement pathway and bind Fc γ receptors
512 upregulated on cells. However further studies will be needed to clarify in TB, how immune
513 complexes form, their composition and the role they play in early disease. Developing a greater
514 understanding of the early events in TB disease will be important to future TB control efforts.
515 Not all those who initially reactivate latent infection and develop evidence of early subclinical
516 disease will go on to develop symptomatic clinical disease, as regression will occur in a
517 proportion. Determining the factors that govern progression or regression of disease will allow
518 us to develop rational interventions that may lead to more favorable outcomes and prevent
519 disease.

520

521 **Materials and Methods**

522 Recruitment of participants

523 Ethical approval for this study was provided by the research ethics committees of the University
524 of Cape Town (013/2011) and Stellenbosch University (N12/11/079). Recruitment and
525 classification of participants whose samples were utilized for this study have been described in
526 detail previously(2). Briefly all participants and controls were HIV-1 infected adults, who were

527 ART naïve and resident in Khayelitsha, a peri-urban township of Cape Town, South Africa
528 where >95% of people are of Xhosa origin. Recruitment took place between 2011 and 2013, TB
529 incidence at the time of the study was >1,000/100,000. All consent documents were provided to
530 potential participants in English or Xhosa and read through with a member of the study team to
531 ensure full understanding and capacity to consent before signing. Participants recruited to
532 undergo PET/CT were recruited in a 2-stage process. At initial screening consent they were
533 provided with an information leaflet in English or Xhosa explaining the study procedures and the
534 risks and benefits of study involvement. At the end of the screening period this leaflet was
535 explained in detail with eligible participants and any queries or concerns addressed prior to final
536 consenting for study entry.

537
538 The 35 asymptomatic participants undergoing FDG-PET/CT had blood sampling for RNA
539 (Tempus, Thermo Fisher Scientific, Waltham, MA) and serum on the day of scan prior to
540 receiving any IPT. The 15 HIV-1 infected controls with symptomatic, microbiologically
541 confirmed pulmonary tuberculosis that were age, sex and CD4 matched to the 35 asymptomatic
542 participants undergoing FDG-PET/CT and had blood sampling for RNA and serum within 24
543 hours of commencing TB treatment but did not undergo FDG-PET/CT.

544 Additional participants were recruited as controls for modular analysis. All were resident in
545 Khayelitsha. All participants were of African ancestry (almost entirely of Xhosa origin).
546 Symptomatic HIV-1 infected and HIV-1 uninfected participants with active TB had their
547 diagnosis confirmed by either a positive sputum culture for Mtb or a positive sputum GeneXpert
548 TB-RIF (Cepheid, Sunnyvale, CA), sputum smear status was also established. Blood sampling
549 of active TB controls was carried out before, or within 24 hours, of treatment commencing.

550 HIV-1 infected participants on ART were established on medication for > 6 months and had a
551 suppressed viral load (<40 copies/mL or lower than detectable limit). Participants were
552 diagnosed HIV-1 infected if they had documented evidence of a positive point of care (POC) test
553 for HIV-1 in their medical notes and, either a positive HIV-1 viral load and/or a positive
554 confirmatory HIV-1 ELISA. HIV-1 uninfected participants had a documented negative POC test
555 for HIV-1. HIV-1 uninfected adults with no evidence of active TB were the main control group
556 for comparison.

557

558 RNA extraction

559 Three mL of blood was drawn into Tempus Blood RNA tubes and shaken vigorously for 10-15
560 seconds. Tempus tubes were stored within 6 hours of sampling in a freezer between 20°C and -
561 80°C for no longer than 21 months before RNA extraction. RNA was extracted using the
562 PerfectPure™ Blood RNA Kit (5 PRIME) according to manufacturer's instructions. RNA
563 integrity was assessed using the Bioanalyser Nano Assay (Agilent, Santa Clara, CA) with all
564 samples having RNA integrity number (RIN) 7-9.5. RNA yield was assessed using a Nanodrop
565 ND 1000 spectrophotometer (Thermoscientific, Waltham, MA) and RNA yield was suboptimal
566 for a single sample (active TB control) that was not analysed.

567 Two thousand nanograms of the isolated total RNA was globin reduced using the Human
568 GLOBINclear™ Kit (Ambion, Austin, TX) according to manufacturer's instructions. 200ng of
569 globin-reduced RNA was then used to prepare and amplify biotinylated, antisense
570 complementary RNA (cRNA) with the TotalPrep RNA Amplification Kit (Illumina, San Diego,
571 CA). 750ng of labelled cRNA was then hybridized overnight to Illumina HumanHT-12 v 4.0
572 Expression BeadChips containing 47,231 probes. Samples were randomly distributed across

573 chips along with control samples to minimize chip related bias. The arrays were washed,
574 blocked, stained and scanned on an Illumina HiScan, as per manufacturer's instructions. Signal
575 intensity values were then generated on Genomestudio (Illumina).

576

577 Microarray data analysis

578 Raw background subtracted expression data was normalized using GeneSpring GX version 12.6
579 (Agilent). For each sample, probes were assigned a signal intensity detection p-value in
580 comparison to background hybridization and probes were assigned a "present" flag using a 0.99
581 cut off. Raw signal values <1 were then set to a threshold of 1 and all values were \log_2
582 transformed. To minimize technical variation, each sample was then normalized using a 75th
583 percentile shift algorithm in which the \log_2 transformed intensity value corresponding to the 75th
584 percentile was subtracted from \log_2 transformed intensity value for each probe within a sample.
585 Baseline transformation was then carried out to rescale intensity values to the median of all
586 samples. Samples were visualized using principal component analysis (PCA) to confirm no
587 outliers. Following this probes that were not "present" in at least 10% of samples were filtered
588 out before further analysis.

589

590 Pathway analysis was conducted on gene lists using Ingenuity Pathway Analysis (IPA) software
591 (Qiagen Bioinformatics, Hilden, Germany). The canonical pathways in IPA are well-
592 characterized metabolic and cell signaling pathways based on the available scientific literature.
593 The strength of association between gene lists and pathways was determined by Fisher's exact
594 test. Where hierarchical clustering was used to visualize data, Pearson uncentered (cosine)
595 distance metric and average linkage rule was used.

596
597 Modular analysis of the transcripts was undertaken. Modules are groups of co-regulated
598 transcripts subsequently categorized into functional groups through unbiased literature review.
599 The principles informing this approach have been previously published (17) as have the specific
600 details of the modules used in this study along with complete transcript lists (36). Extensive
601 functional analysis of these modules using a variety of analytic approaches are available through
602 the following link http://www.biiir.net/public_wikis/module_annotation/V2_Trial_8_Modules).
603 The average transcript abundance for each module was determined for each participant. Of the
604 260 modules, 38 had functional roles determined and analysis was restricted to these modules.
605 HIV-1 uninfected adults with no evidence of active TB were used as the primary control group.
606 The *Simes-Benjamini-Hochberg* method was used to control for false discovery rate (FDR) in
607 analysis of modules

608
609 The raw and normalized microarray data has been deposited in GEO (GSE69581). All data
610 collected and analyzed in the experiments adhere to the Minimal Information About a
611 Microarray Experiment (MIAME) guidelines.

612
613 *RNA sequence data analysis from Zak et al*
614 Sequencing data was downloaded from NCBI GEO repository with project number
615 PRJNA315611. Metadata was provided in GEO repository and supplementary data of associated
616 publication(16). 93 samples were available from progressors. Per protocol time to TB was used
617 to categorise each sample as being taken <180 days, 181-360 days, 361-540 days, 541-720 days,
618 >720 days prior to diagnosis or being taken after diagnosis. Samples taken after diagnosis or
619 more than 720 days before diagnosis were not included in analysis leaving 72 samples from

620 progressors across four timepoints. In order to allow for determination of differentially
621 expressed genes at each of the four timepoints, four groups of non-progressors were assigned in a
622 1:1 ratio ensuring matching by time from recruitment (**see Supp Excel sheet**). All sequence data
623 were quality checked with FastQC (version 0.11.5) before being aligned to the human genome
624 (NCBI GRCh38.p10 build) using STAR (version 2.5.2b) with default parameters. Gene counting
625 of the position-sorted aligned reads was done using HTSeq-count (version 0.6.1p1) with the
626 default union mode. All genes with <1 reads on average across all samples were filtered out from
627 expression analysis. Read count normalisation and differential gene expression analysis was
628 done using DESeq2 in R (37) and the fold change and false discovery rate corrected significance
629 (adjusted p-value) for each gene between progressors and non-progressors are reported.

630

631 RT-PCR arrays

632 RNA extracted from whole blood used for the microarrays was reverse transcribed using the RT²
633 First Strand Kit (Qiagen, Hilden, Germany) which includes a genomic DNA (gDNA) elimination
634 step. cDNA was analysed using 384-well RT² Profiler Custom PCR Arrays (Qiagen, Hilden,
635 Germany) on the Roche 480 platform. The arrays included 4 house keeping (HK) genes (*HPRT1*,
636 *B2M*, *RPLP0*, *HSP90AB1*), three control reactions to monitor gDNA contamination and reverse
637 transcription efficiency, and the genes of interest (including *CIQB*, *FCGBP*, *FCGRI*,
638 *SERPING1*). Delta Ct (ΔCt) was calculated according to the average Ct of the 4 HK genes. Delta
639 delta Ct ($\Delta\Delta Ct$) was calculated as the sample ΔCt -Median ΔCt of all samples, and fold change
640 was calculated as $2^{(-\Delta\Delta Ct)}$. Log₂ normalised fold change values (mean=0, variance=1) were
641 plotted as box plots in Qlucore Omics explorer.

642

643 Serum analysis

644 Blood was drawn into 5mL SST™ II Advance tubes (BD Diagnostics, Franklin Lakes, NJ),
645 transported to the laboratory and centrifuged at 1200g for 10 minutes. The serum was aliquoted
646 and stored at -80°C. Two of 15 active TB participants had no serum available. All 35
647 participants that underwent FDG-PET/CT had serum available. Analytes were measured by
648 ELISA: SerpinG1 (Cusabio, Wuhan, China), Circulating Immune complex (Bühlmann, Bremen,
649 Germany), C1q (Abcam, Cambridge, UK), C5 (assay measures uncleaved C5 and C5a) (Abcam,
650 Cambridge, UK). ELISA plates were read on a Bio-Rad iMark microplate reader (Bio-Rad,
651 Hercules, CA, USA) with standard curves generated for each analyte. Values that were below
652 manufacturer determined minimal detectable limit or the minimum asymptote of the standard
653 curve were assigned a zero value.

654

655 Statistical Analysis

656 Apart from microarray data where analysis was conducted primarily in GeneSpring GX version
657 12.6 (Agilent) and by Ingenuity Pathway Analysis software (Qiagen) as described above,
658 statistical analysis of continuous and categorical variables, correlation analysis and data
659 visualization was conducted in Stata ver. 12.1 (StataCorp) and Prism ver. 7.0c (GraphPad
660 software). The normality of data was assessed by the Shapiro-Wilk test and variance compared
661 by F-test or Bartlett's test. Non-parametric data was compared using the Mann-Whitney *U* test
662 or the Kruskal Wallis test and parametric data compared using t-test or ANOVA. Two-stage
663 linear step-up procedure of Benjamini, Krieger and Yekutieli was to control for false discovery
664 rate following Kruskal Wallis test if needed. Correlation was performed by Spearman rho or

665 Pearson's test depending on distribution of data. Proportions were compared by χ^2 test or
666 Fisher's exact test (if the contingency included a number ≤ 5).

667 **Author Contributions**

668 R.J.W., H.E., C.E.B. and A.O'G. designed the study; H.E., R.P.L. and C.M.G. processed whole
669 blood for microarray experiments; H.E., R.P.L, S.H. and M.L. analyzed transcriptomic data, with
670 advice and input from C.M.G., A.K.C. and A.O'G.; H.E. and K.A.W. performed serum studies;
671 A.K.C performed and analyzed RT-PCR; M.L. conducted additional statically analyses; R.J.W.
672 supervised data analysis; H.E. and R.J.W wrote the manuscript and subsequently all authors
673 provided advice and approved the final manuscript.

674

675 **Acknowledgements**

676 We thank all participants, clinic and laboratory staff for invaluable assistance. We also thank
677 Douglas B Young of the Francis Crick Institute for early discussion around study design and
678 analysis. This work was funded by the Wellcome Trust (090170, 203135, 104803), the Bill and
679 Melinda Gates Foundation/Wellcome Trust Grand challenges in Global Health (37822), the
680 intramural research program of NIH/NIAID and the National Institutes of Health (R01
681 HL106804). RJW is supported by the Francis Crick Institute that receives its core funding from
682 Cancer Research UK (FC00110218), the UK Medical Research Council (FC00110218), and the
683 Wellcome Trust (FC00110218). R.J.W. also received support from the European Union (FP7
684 HEALTH F3-2012-305578), National Research Foundation of South Africa (96841) and
685 Medical Research Council of South Africa (SHIP-02-2013). A.O'G is also supported by the
686 Francis Crick Institute. A.K.C is supported by the Medical Research Council of South Africa

687 (SHIP-02-2013) and the National Institutes of Health TB Research Unit 1U19AI111276 (TBRU-
688 BURU).

689

690 **References**

691 1. Esmail H, Barry CE, 3rd, Young DB, Wilkinson RJ (2014) The ongoing challenge of
692 latent tuberculosis. *Philos Trans R Soc Lond B Biol Sci* 369(1645):20130437.

693 2. Esmail H, Lai RP, Lesosky M, Wilkinson KA, Graham CM, *et al.* (2016)
694 Characterization of progressive HIV-associated tuberculosis using 2-deoxy-2-[18F]fluoro-D-
695 glucose positron emission and computed tomography. *Nat Med* 22(10):1090-3.

696 3. Loveday M, Ramjee A, Osburn G, Master I, Kabera G, *et al.* (2017) Drug-resistant
697 tuberculosis in patients with minimal symptoms: favourable outcomes in the absence of
698 treatment. *Int J Tuberc Lung Dis* 21(5):556-63.

699 4. Lin PL, Ford CB, Coleman MT, Myers AJ, Gawande R, *et al.* (2014) Sterilization of
700 granulomas is common in active and latent tuberculosis despite within-host variability in
701 bacterial killing. *Nat Med* 20(1):75-9.

702 5. Hunter RL (2011) Pathology of post primary tuberculosis of the lung: An illustrated
703 critical review. *Tuberculosis* 91(6):497-509.

704 6. Steinbruck P, Dankova D, Edwards LB, Doster B, Livesay VT (1972) Tuberculosis risk
705 in persons with "fibrotic" x-ray lesions. *Bull Int Union Tuberc* 47:135-59.

- 706 7. Koppaka R, Bock N. How reliable is chest radiography? In: Frieden T, editor. Toman's
707 tuberculosis case detection, treatment, and monitoring: questions and answers. Geneva: World
708 Health Organization; 2004. p. 51-60.
- 709 8. Mamede M, Higashi T, Kitaichi M, Ishizu K, Ishimori T, *et al.* (2005) [18F]FDG uptake
710 and PCNA, Glut-1, and Hexokinase-II expressions in cancers and inflammatory lesions of the
711 lung. *Neoplasia* 7(4):369-79.
- 712 9. Jacobsen M, Repsilber D, Gutschmidt A, Neher A, Feldmann K, *et al.* (2007) Candidate
713 biomarkers for discrimination between infection and disease caused by *Mycobacterium*
714 *tuberculosis*. *J Mol Med* 85(6):613-21.
- 715 10. Maertzdorf J, Repsilber D, Parida SK, Stanley K, Roberts T, *et al.* (2011) Human gene
716 expression profiles of susceptibility and resistance in tuberculosis. *Genes Immun* 12(1):15-22.
- 717 11. Berry MP, Graham CM, McNab FW, Xu Z, Bloch SA, *et al.* (2010) An interferon-
718 inducible neutrophil-driven blood transcriptional signature in human tuberculosis. *Nature*
719 466(7309):973-7.
- 720 12. Kaforou M, Wright VJ, Oni T, French N, Anderson ST, *et al.* (2013) Detection of
721 tuberculosis in HIV-infected and -uninfected African adults using whole blood RNA expression
722 signatures: a case-control study. *PLoS Med* 10(10):e1001538.
- 723 13. Blankley S, Graham CM, Levin J, Turner J, Berry MP, *et al.* (2016) A 380-gene meta-
724 signature of active tuberculosis compared with healthy controls. *Eur Respir J* 47(6):1873-6.

- 725 14. Blankley S, Graham CM, Turner J, Berry MP, Bloom CI, *et al.* (2016) The
726 Transcriptional Signature of Active Tuberculosis Reflects Symptom Status in Extra-Pulmonary
727 and Pulmonary Tuberculosis. *PLoS ONE* 11(10):e0162220.
- 728 15. Walport MJ (2001) Complement. Second of two parts. *N Engl J Med* 344(15):1140-4.
- 729 16. Zak DE, Penn-Nicholson A, Scriba TJ, Thompson E, Suliman S, *et al.* (2016) A blood
730 RNA signature for tuberculosis disease risk: a prospective cohort study. *Lancet* 387:2312-22.
- 731 17. Chaussabel D, Quinn C, Shen J, Patel P, Glaser C, *et al.* (2008) A modular analysis
732 framework for blood genomics studies: application to systemic lupus erythematosus. *Immunity*
733 29(1):150-64.
- 734 18. Bloom CI, Graham CM, Berry MP, Rozakeas F, Redford PS, *et al.* (2013)
735 Transcriptional blood signatures distinguish pulmonary tuberculosis, pulmonary sarcoidosis,
736 pneumonias and lung cancers. *PLoS ONE* 8(8):e70630.
- 737 19. Maertzdorf J, Weiner J, 3rd, Mollenkopf HJ, Bauer T, Prasse A, *et al.* (2012) Common
738 patterns and disease-related signatures in tuberculosis and sarcoidosis. *Proc Natl Acad Sci U S A*
739 109(20):7853-8.
- 740 20. Cliff JM, Lee JS, Constantinou N, Cho JE, Clark TG, *et al.* (2013) Distinct phases of
741 blood gene expression pattern through tuberculosis treatment reflect modulation of the humoral
742 immune response. *J Infect Dis* 207(1):18-29.

- 743 21. Raja A, Ranganathan UD, Ramalingam B (2006) Clinical value of specific detection of
744 immune complex-bound antibodies in pulmonary tuberculosis. *Diagn Microbiol Infect Dis*
745 56(3):281-7.
- 746 22. Raja A, Narayanan PR, Mathew R, Prabhakar R (1995) Characterization of
747 mycobacterial antigens and antibodies in circulating immune complexes from pulmonary
748 tuberculosis. *J Lab Clin Med* 125(5):581-7.
- 749 23. Lu LL, Chung AW, Rosebrock TR, Ghebremichael M, Yu WH, *et al.* (2016) A
750 Functional Role for Antibodies in Tuberculosis. *Cell* 167(2):433-43.
- 751 24. Kozakiewicz L, Phuah J, Flynn J, Chan J (2013) The role of B cells and humoral
752 immunity in Mycobacterium tuberculosis infection. *Adv Exp Med Biol* 783:225-50.
- 753 25. Nimmerjahn F, Ravetch JV (2008) Fcγ receptors as regulators of immune
754 responses. *Nat Rev Immunol* 8(1):34-47.
- 755 26. Welsh KJ, Risin SA, Actor JK, Hunter RL (2011) Immunopathology of postprimary
756 tuberculosis: increased T-regulatory cells and DEC-205-positive foamy macrophages in cavitary
757 lesions. *Clin Dev Immunol* 2011:307631.
- 758 27. Hunter RL, Actor JK, Hwang SA, Karev V, Jagannath C (2014) Pathogenesis of post
759 primary tuberculosis: immunity and hypersensitivity in the development of cavities. *Ann Clin*
760 *Lab Sci* 44(4):365-87.
- 761 28. Hunter RL (2016) Tuberculosis as a three-act play: A new paradigm for the pathogenesis
762 of pulmonary tuberculosis. *Tuberculosis* 97:8-17.

- 763 29. Raja A, Baughman RP, Daniel TM (1988) The Detection by Immunoassay of Antibody
764 to Mycobacterial Antigens and Mycobacterial Antigens in Bronchoalveolar Lavage Fluid from
765 Patients with Tuberculosis and Control Subjects. *Chest* 94(1):133-7.
- 766 30. Kobayashi K, Ogata H, Morikawa M, Iijima S, Harada N, *et al.* (2002) Distribution and
767 partial characterisation of IgG Fc binding protein in various mucin producing cells and body
768 fluids. *Gut* 51(2):169-76.
- 769 31. Larsen GL, Mitchell BC, Henson PM (1981) The pulmonary response of C5 sufficient
770 and deficient mice to immune complexes. *Am Rev Respir Dis* 123(4 Pt 1):434-9.
- 771 32. Schifferli JA, Ng YC, Peters DK (1986) The role of complement and its receptor in the
772 elimination of immune complexes. *N Engl J Med* 315(8):488-95.
- 773 33. Schifferli JA, Peters DK (1983) Complement, the immune-complex lattice, and the
774 pathophysiology of complement-deficiency syndromes. *Lancet* 2(8356):957-9.
- 775 34. Cai Y, Yang Q, Tang Y, Zhang M, Liu H, *et al.* (2014) Increased complement C1q level
776 marks active disease in human tuberculosis. *PLoS ONE* 9(3):e92340.
- 777 35. Morgan BP, Gasque P (1997) Extrahepatic complement biosynthesis: where, when and
778 why? *Clin Exp Immunol* 107(1):1-7.
- 779 36. Obermoser G, Presnell S, Domico K, Xu H, Wang Y, *et al.* (2013) Systems scale
780 interactive exploration reveals quantitative and qualitative differences in response to influenza
781 and pneumococcal vaccines. *Immunity* 38(4):831-44.

782 37. Love MI, Huber W, Anders S (2014) Moderated estimation of fold change and dispersion
783 for RNA-seq data with DESeq2. *Genome Biol* 15(12):550.

784

785

786

787

788

789

790

791

792

793

794

795

796

797

798

799

800

801

802

803

804

805

806

807

808

809

810

811

812

813

814

815

816

817

818

819

820

821

822

823

824

825

826

827

828

829

830

Figure 1

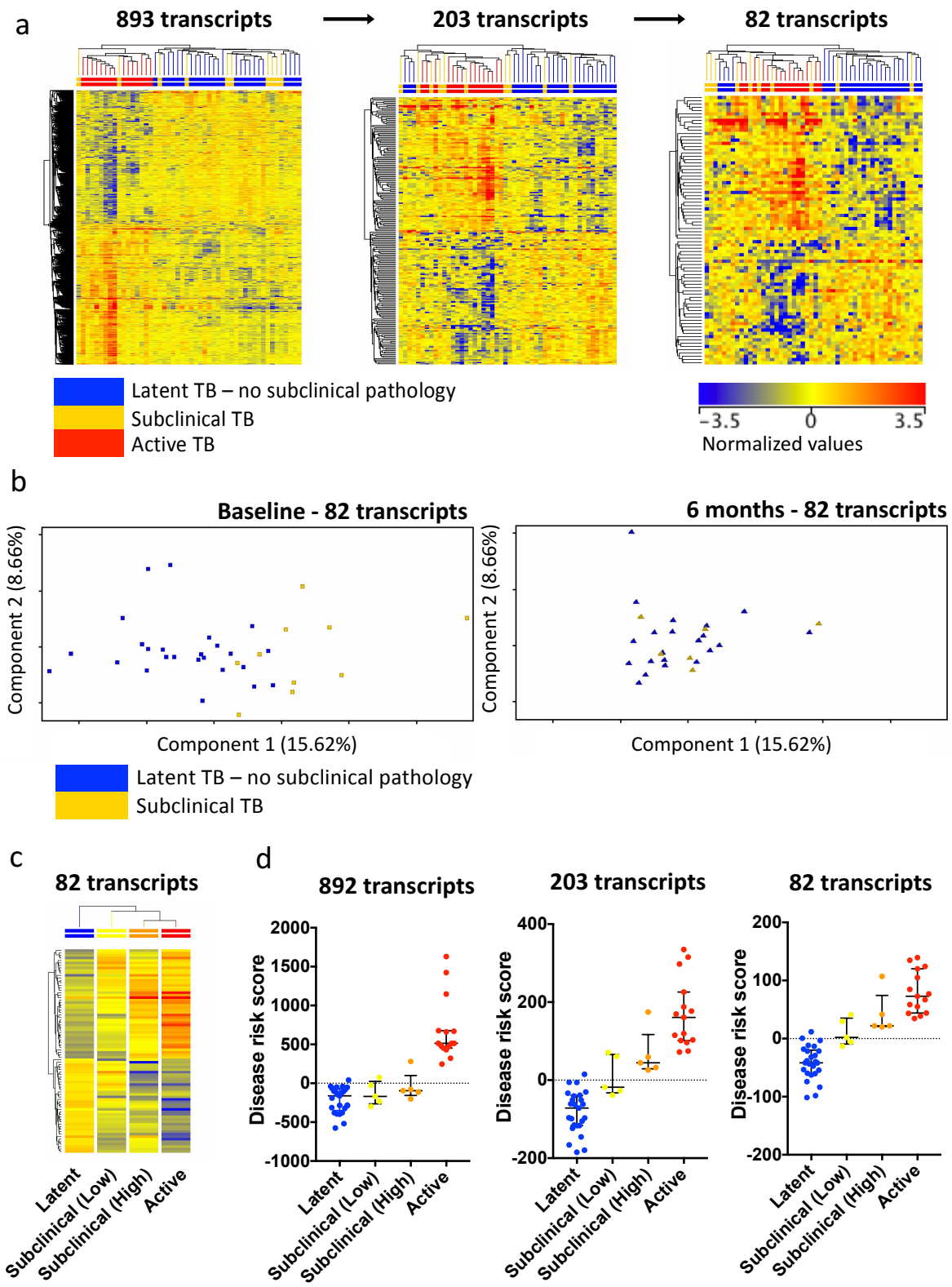


Figure 2

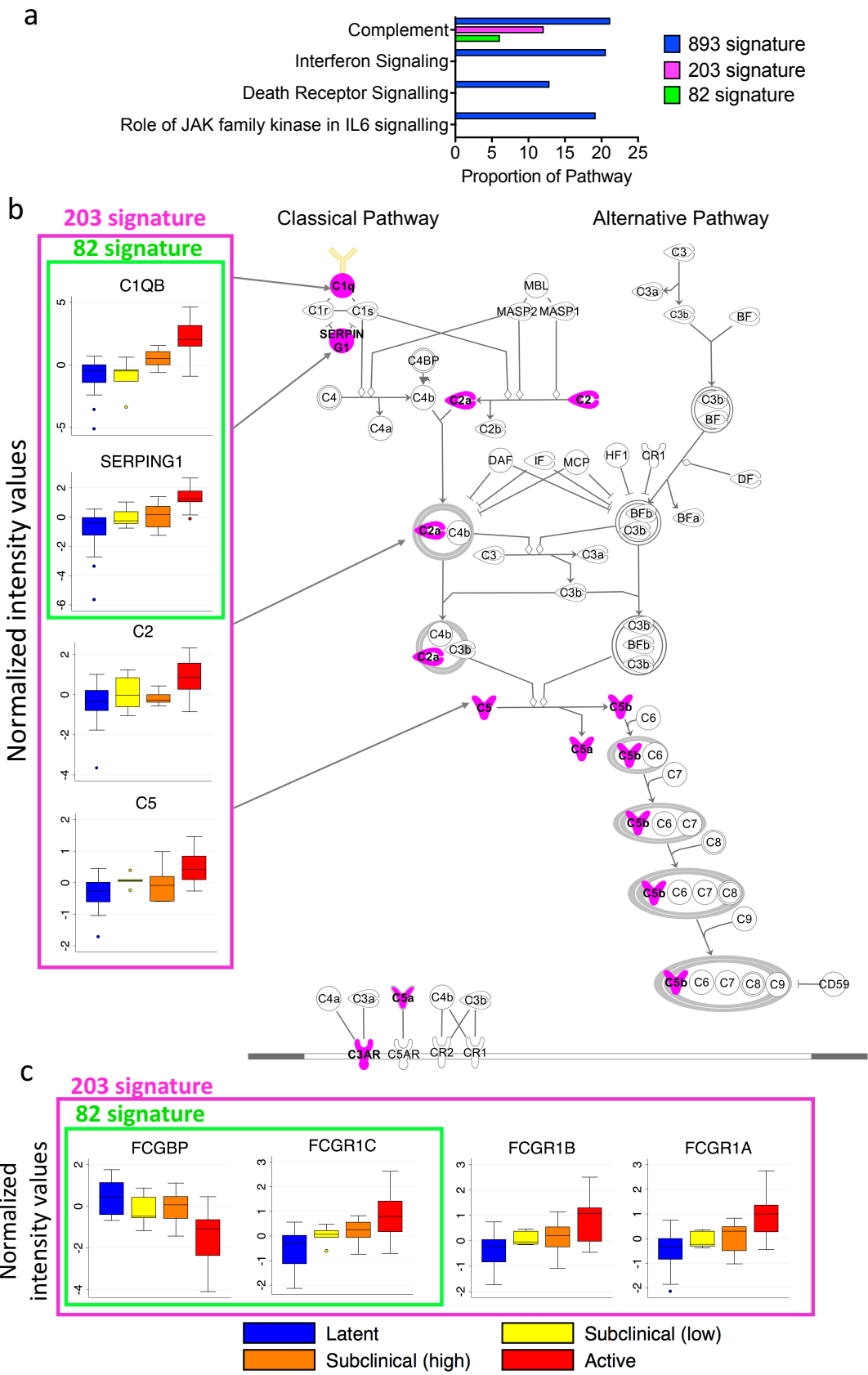


Figure 3

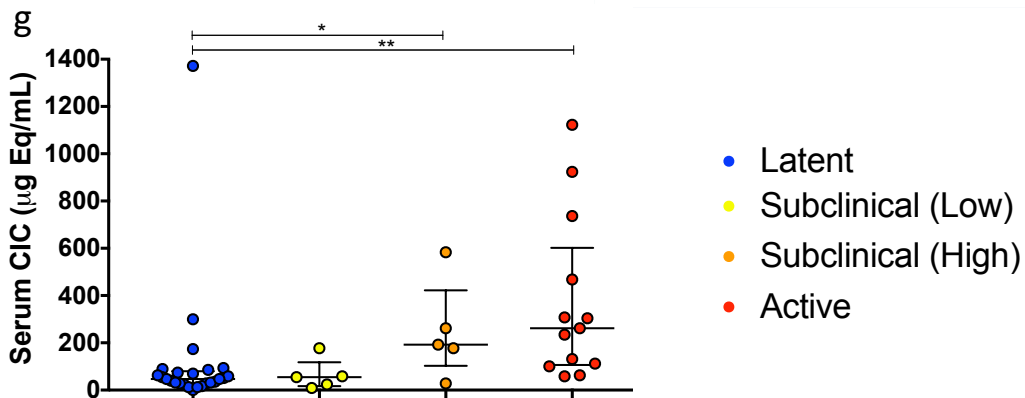
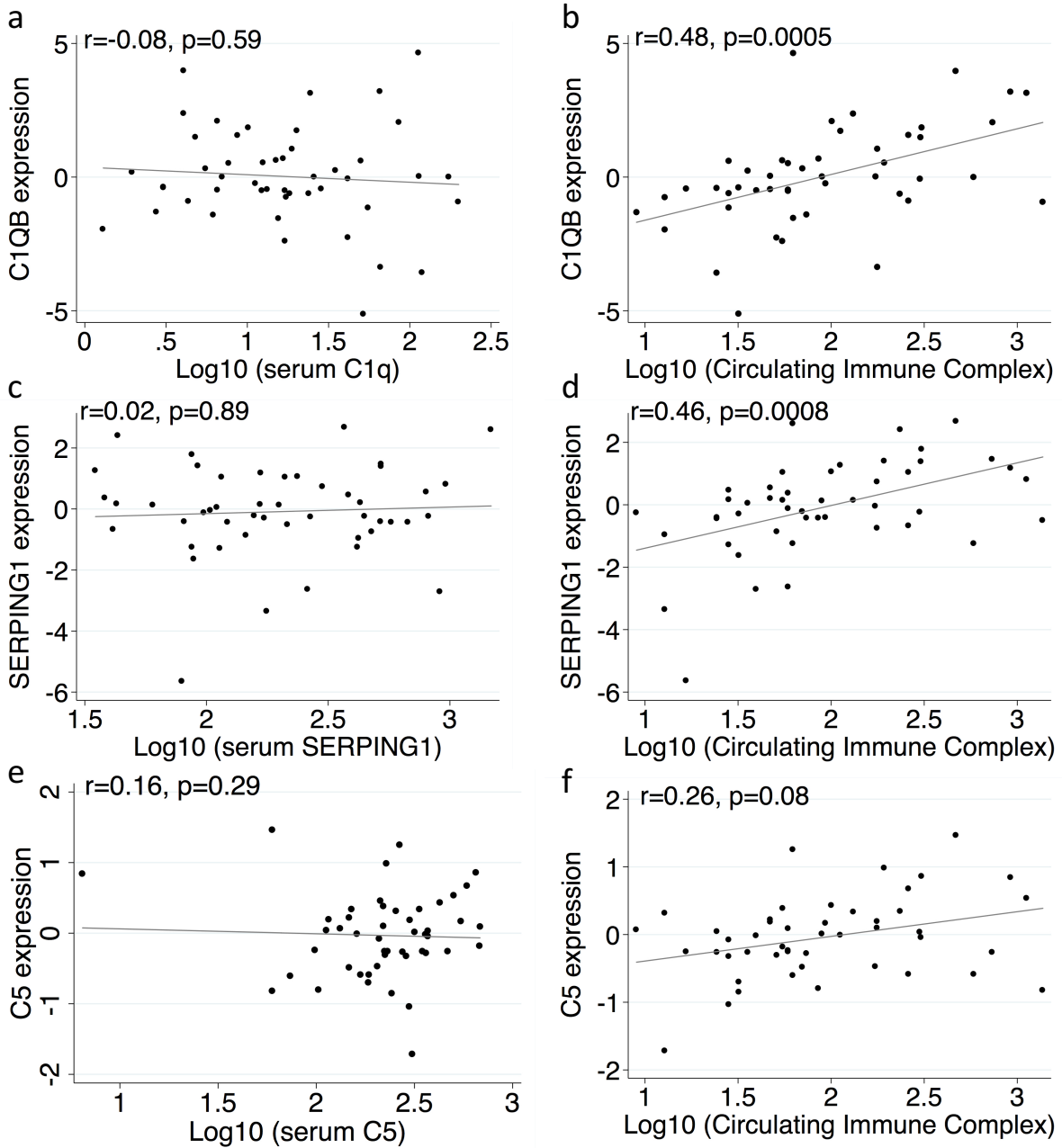


Figure 4

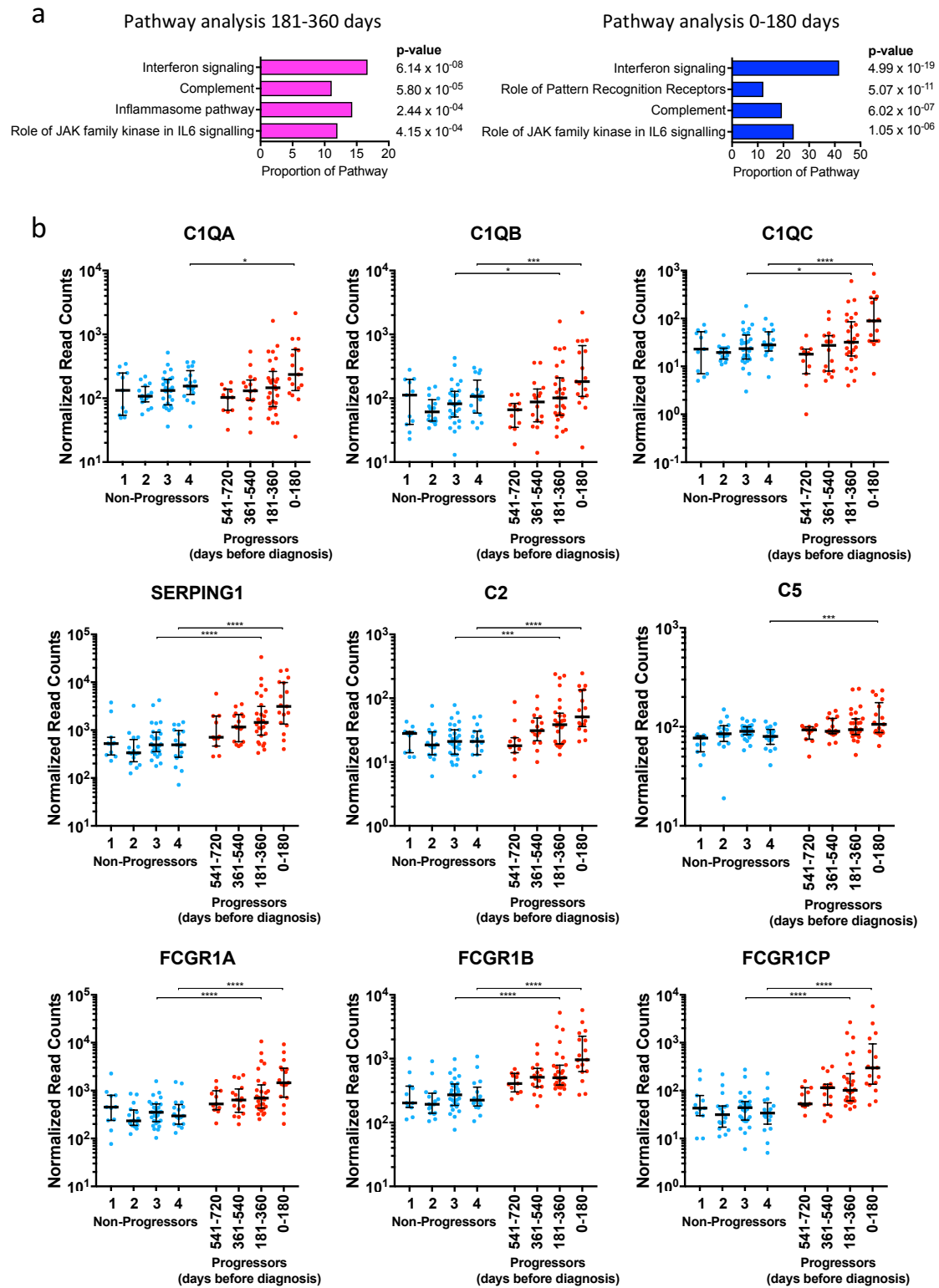
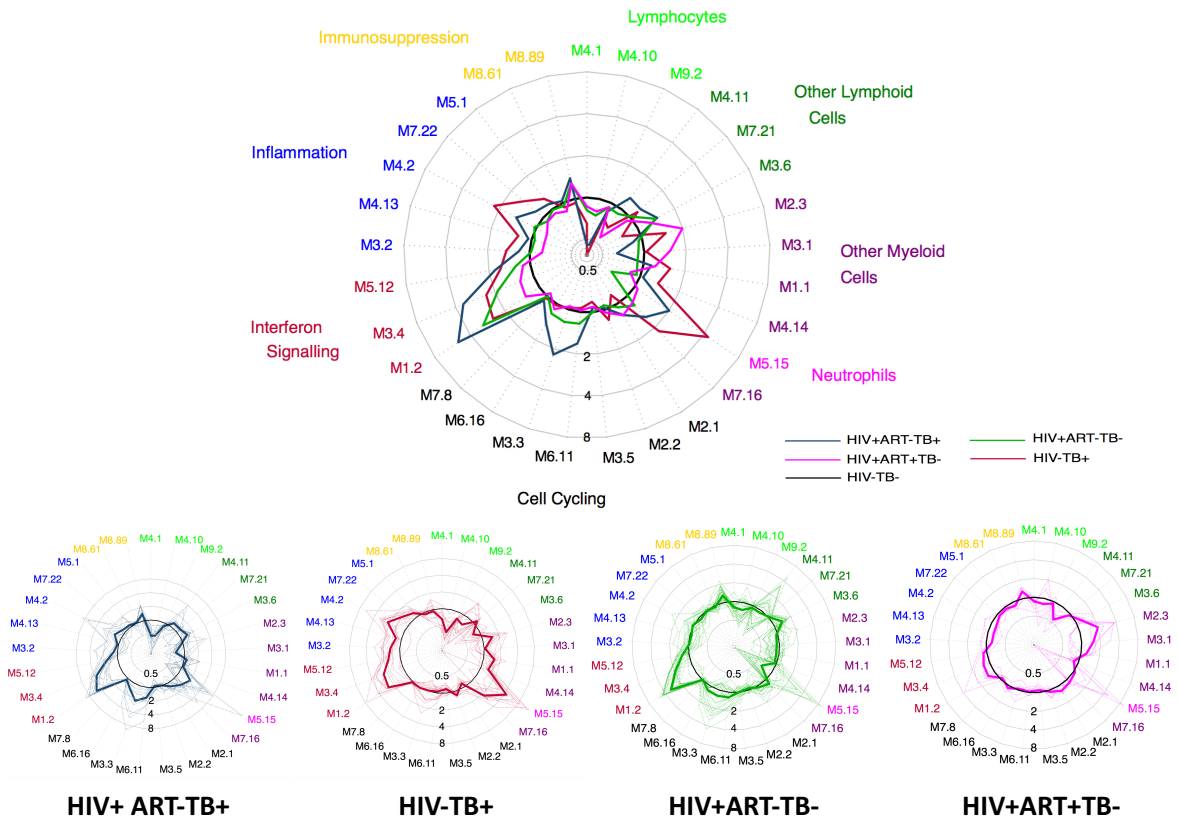


Figure 5



836 **Figure Legends**

837

838 **Figure 1**

839 **Statistical and fold change filtering reveals 82 transcripts that separate active and**
840 **subclinical TB from latent TB**

841 **a.** Heatmaps showing hierarchical clustering (Pearson Uncentered (cosine) distance metric and
842 average linkage rule) for the 893, 203 and 82 transcript signatures. Active TB (n=15, red),
843 Subclinical TB (n=10, orange), Latent TB (n=25, blue), showing increasing clustering of
844 subclinical TB with active TB and increasing separation of subclinical TB from latent TB (with
845 no subclinical pathology).

846

847 **b.** 2D-PCA plot showing effect of treatment on 82 transcripts. Left panel shows pre-treatment,
848 with separation seen between subclinical TB (n=10) represented as orange squares and latent TB
849 (with no evidence of subclinical pathology) (n=25) as blue squares. In the right panel post
850 treatment (for 27 of 35 participants) those with previous subclinical TB (n=6) (orange triangle)
851 cluster with latent TB (n=21) (blue triangles).

852

853 **c.** Subclinical TB cases with higher metabolic activity on FDG-PET/CT clustered more closely
854 with active TB. Participants with subclinical TB (n=10) were subclassified into those with low
855 intensity FDG uptake within lung parenchymal or mediastinal lymph nodes (Visual Score 0-1 –
856 FDG uptake less than or equal to mediastinal blood pool, Yellow – n=5) or high intensity uptake
857 (Visual Score 3 – FDG uptake greater than mediastinal blood pool, Orange – n=5). Participants
858 with active TB (n=15) are shown in Red and with latent TB (n=25) in Blue. Heatmap (c)

859 represents average expression within the 4 groups for each of the 82-transcripts and shows
860 hierarchical clustering (Pearson Uncentered (cosine) distance metric and average linkage rule).
861 Participants with subclinical TB and high intensity FDG uptake were more closely related to
862 Active TB.

863

864 **d.** A Disease risk score was determined for each participant using the 893, 203 and 82 transcripts
865 by subtracting the summed normalized expression values of under-abundant transcripts from that
866 of over-abundant transcripts (see (12)). A dot plot was used to visualize differences between the
867 groups

868

869 **Figure 2**

870 **Transcripts relating to the classical complement pathway are overabundant in**
871 **subclinical and active TB.**

872 **a.** Top 4 enriched canonical pathways listed by significance ($p < 0.05$, Fisher's exact) for the 893-
873 transcript signature of active TB shown. The bar chart shows the proportion of these pathways
874 represented in the 893, 203 and 82-transcript signatures.

875

876 **b.** Schematic of the complement pathway, created using Ingenuity Pathway Analysis software,
877 showing components of the pathway with overabundant transcripts in active ($n=15$) and
878 subclinical TB ($n=10$) compared to latent TB ($n=25$) (in pink). Box and whisker plots show
879 normalized expression of complement components SERPING1 and C1QB (part of 82-transcript
880 signature) and C2 and C5 (part of 203- transcript signature) by TB disease state.

881

882 c. Box and whisker plots show normalized expression of immunoglobulin related transcripts
883 FCGBP and FCGR1C (part of 82-transcript signature) and FCGR1A and FCGR1B (part of 203-
884 transcript signature) by TB disease state.

885

886 **Figure 3**

887 **Correlation of transcript abundance with serum concentration of complement components** 888 **and Circulating Immune Complex**

889 a-f. Scatter plots showing correlation of transcript abundance against serum concentration of
890 protein product with Spearman rho and p-value for; (a) C1QB transcript abundance vs C1q
891 serum concentration, (b) C1QB transcript abundance vs serum circulating immune complex
892 (CIC) concentration, (c) SERPING1 transcript abundance vs. SERPING1 serum concentration,
893 (d) SERPING1 transcript abundance vs serum CIC concentration, (e) C5 transcript abundance vs
894 C5 serum concentration, (f) C5 transcript abundance vs serum CIC concentration. Correlation
895 was calculated for 48 participants with serum samples (13 active TB (as 2 of 15 participants did
896 not have serum available), 10 subclinical TB and 25 latent TB). For graphs b, d and f, a single
897 outlier with serum circulating immune complex concentration below detectable limit is not
898 shown.

899

900 g. Dot plot with median and IQR showing the CIC level for participants with latent, subclinical
901 (low activity), subclinical (high activity) and active TB. CIC was significantly increased across
902 different TB disease states ($p=0.0004$ - Kruskal Wallis), *post hoc* analysis controlling for false
903 discovery by Two-stage linear step-up procedure of Benjamini, Krieger and Yekutieli
904 demonstrated that those with active TB ($p=0.0001$, $q=0.0002$) and those with subclinical TB and

905 high metabolic activity on PET/CT ($p=0.038$, $q=0.04$) had higher serum concentration of CIC
906 than latent TB

907

908 **Figure 4**

909 **Complement and Fc Gamma receptor genes significantly differentially expressed between**
910 **progressors and non-progressors from Zak *et al***

911 Analysis of RNAseq data for HIV uninfected persons who eventually progressed to TB in
912 comparison to matched non-progressors from Zak *et al*. Genes with <1 read on average across
913 all samples were filtered out with expression analysis therefore conducted on 25,518 genes (see
914 methods). 892 genes were significantly differentially abundant ($p_{\text{corr}} < 0.05$) between progressors
915 0-180 days prior to diagnosis and matched non-progressors, of which 362 were also >1.5 fold
916 overabundant. 610 genes were significantly differentially abundant ($p_{\text{corr}} < 0.05$) between
917 progressors 181-360 days prior to diagnosis and matched non-progressors, of which 154 were
918 also >1.5 fold overabundant. IPA pathway analysis was conducted on these gene lists.

919

920 **a.** Top 4 enriched canonical pathways listed by significance ($p < 0.05$, Fisher's exact) for the 362
921 genes and 154 genes differentially abundant at 0-180 and 181-360 days prior to diagnosis. The
922 bar chart shows the proportion of these pathways represented.

923

924 **b.** Dot plots showing gene abundance (as normalized read counts) in progressors in 180 day
925 blocks prior to disease presentation in comparison to 1:1 matched non-progressors (labeled 1-4
926 see methods and Supp Excel sheet)). All components of the complement pathway or Fc gamma
927 receptor within the group of significantly differentially abundant at either <180 days or 181-360

928 days before diagnosis are shown. Significance shown by asterisk; $p_{\text{corr}} < 0.05$ (*), < 0.01 (**),
929 < 0.001 (***), < 0.0001 (****) (see Supp Excel sheet for exact values)

930

931 **Figure 5**

932 **Comparison of modular transcript abundance by TB and HIV status**

933 **a** – Radar plots depicting fold change in transcript abundance in comparison to median modular
934 transcript abundance in control group (HIV- TB-) for 29 modules. Plot on left shows fold
935 change of median modular transcript abundance for HIV+ART-TB- (green), HIV- TB+ (red),
936 HIV+ART- TB+ (blue) and HIV+ART+TB- (pink) in comparison to HIV-TB- controls (black)
937 overlaid on same graph Plots on right show fold change for each individual participant in the
938 four groups in comparison to control (HIV- TB-) with the median value in bold. Log₂ scale..
939 See also Supp table 3.

940

941

942

943

944

945

946

947

948

949

950

951

952

953

954

955